Algae through the looking glass

Journal:	*Microscopy Research and Technique*
Manuscript ID	Draft
Wiley - Manuscript type:	Review Article
Date Submitted by the Author:	n/a
Complete List of Authors:	Coltelli, Primo Barsanti, Laura Evangelista, Valter Gualtieri, Paolo; CNR Biofisica;
Keywords:	microalgae; automatic identification; automatic track reconstruction; microspectroscopy, digital microscopy.

Algae through the looking glass

Primo Coltelli[1], Barsanti Laura[2], Valter Evangelista[3], and Gualtieri Paolo[4*]

[1] Istituto Scienza e Tecnologie dell'Informazione, CNR, Via Moruzzi 1, 56124 Pisa; primo.coltellil@isti.cnr.it
[2] Istituto di Biofisica, CNR, Via Moruzzi 1, 56124 Pisa; laura.barsanti@pi.ibf.cnr.it
[3] Istituto di Biofisica, CNR, Via Moruzzi 1, 56124 Pisa; valter.evangelista@pi.ibf.cnr.it
[4] Istituto di Biofisica, CNR, Via Moruzzi 1, 56124 Pisa; paolo.gualtieri@pi.ibf.cnr.it

* Correspondence: e-mail: paolo.gualtieri@pi.ibf.cnr.it; Tel.: +39 050 315 3026

Running Head: Algae through the looking glass

Abstract

Microalgae are one of the most suitable subjects for testing the potentiality of light microscopy and image analysis, because of the size of single cells, their endogenous chromaticity, and their metabolic and physiological characteristics. Microscope observations and image analysis can use microalgal cells from lab cultures or collected from water bodies as model to investigate metabolic processes, behavior/reaction of cells under chemical or photic stimuli, and dynamics of population in the natural environment in response to changing conditions. In this paper we will describe the original microscope we set up together with the image processing techniques we improved to deal with these topics. Our system detects and recognizes in-focus cells, extracts their features, measures cell concentration in multi-algal samples, reconstructs swimming cell tracks, monitors metabolic processes, and measure absorption and fluorescent spectra of subcellular compartments. It can be used as digital microscopy station for algal cell biology and behavioral studies, and field analysis applications.

Keywords: micr**o**algae; automatic identification; automatic track reconstruction; microspectroscopy, digital microscopy.

Research Highlight

- monitoring of Cr^{6+} effect on algae chloroplasts and analysis of movement parameters of swimming algae;
- spectroscopic dynamics of *Euglena* photoreceptor;
- water monitoring station to follow algae population dynamics in natural environment.

Authors declare no conflict of interest

1. Introduction

Microalgae possess the perfect size, color and physiology to be an elective subject for light microscopy and image processing. They can serve as model to investigate the metabolic processes and behavior/reaction of a cell under chemical or photic stimuli, or determine the dynamic of natural populations in response to variations of environmental conditions. In fact, algae can occasionally bloom in enormous amount becoming a serious public health and environmental problem (Artiola, et al., 2004; Barsanti and Gualtieri, 2014; Wiersma, 2004).

Light microscopy allows imaging and processing of proteins and algal cells under both lab controlled conditions and natural environment (Gualtieri, 1992); when microscopes are coupled with special set-ups and appropriate image analysis processing routines, they can produce five dimensional images. In fact, wavelength (λ) and time (t) add to the common three space coordinates, x, y, and z, allowing the measurement of absorption/fluorescence spectra and time lapse image sequences (Barsanti, et al., 1997; Barsanti, et al., 2007; Evangelista, et al., 2003; Evangelista, et al., 2006; Gualtieri, et al., 1989a; Gualtieri, et al., 1989b; Gualtieri, 1991; Walker et al., 2002). Absorption and fluorescence spectra give a reliable and *in vivo* picture of the metabolic processes dynamics under physiological conditions and/or in response to environmental stressors (Juarez, et al., 2008; Rodriguez, et al., 2007). Time analysis is mandatory in the study of integrate biological processes such as the study on the behavior of algae under different external stimuli (light or chemical). The exact determination of the motion parameters of swimming microalgae, performed in real time, can provide measurements with reliable statistics of the physiological aspects of cellular integrated responses (Barsanti, et al., 2016; Gualtieri, et al., 1988). Moreover, in the natural environment, light microscopy enables us to monitor algal bloom composition and dynamics, essential to detect early warning signs of critical conditions for a safe management of water bodies and resources (Carvalho, et al., 2013; Evangelista, et al., 2008; Rai, et al., 2008; Singh, et al., 2013). Therefore, image processing techniques, coupled to original microscope set-ups, can provide deterministic solutions, automatically and in quasi-real-time.

In this paper we will deal with algae as either cell models or environmental probes, and describe four experimental cases on which our system has been tested. The four cases are:

1. monitoring of Cr^{6+} effect on the chloroplasts of *Chlamydomonas reinhardtii, Eudorina unicocca* and *Chlorella kessleri*;
2. analysis of the movement parameters of swimming algae under external stimuli;
3. spectroscopic dynamics of *Euglena gracilis* photoreceptor functioning;
4. realization of a water monitoring station that automatically detects, recognizes, identifies and enumerates genera and species of microalgae belonging to all the algal divisions.

2. Materials and Methods

Algae slides are acquired by means of a home-made microscopy set-up (Figure 1) and the digital data are processed to obtain a deterministic solution of the different cases. A Zeiss Axioplan microscope (Zeiss, Germany), equipped with a tungsten lamp regulated at 100 W (3200 K) (Figure 1a), an oil immersion condenser (Figure 1b), and planapochromatic objectives (Figure 1d) was used for *in vivo* and real time image analysis and microspectroscopy. An epi-fluorescent system, consisting of a 100W mercury lamp and different sets of filters combinations (Zeiss, Germany), can be mounted onto the microscope (not shown in Figure 1 for sake of clarity). The microscope has both a manual and a motorized mechanical 75x30 mm scanning stage (Märzhäuser, Wetzlar, Germany) driven by a stepper motor controller (Figure 1c). The microscope is set at the best performance of Koehler illumination requirements (Zieler, 1972). A two-ports binocular tube (Zeiss, Germany) (Figure 1e) mounted onto the microscope houses either a CCD camera (Basler scA160028fm/fc, Basler, Germany; IEEE 1394b interface) or a CMOS camera at 500 frames/s (Photron, Fastcam SA3, San Diego, USA; gigabit Ethernet interface) (Figure 1f) in the front port; and a high quality inspection probe (model 77423, Oriel, Stratford, Connecticut, USA) in the back focal plane of the rear port (Figure 1g). The personal computer is an Intel Core i7, 16GB 1600MHz DDR3 ram memory, and 2 TB HD.

For correct color acquisition, the CCD camera undergoes color calibration in three steps: White balancing, Gamma correction, and Matrix correction (Coltelli, et al., 2016). For integrated density determination, quasi-monochromatic images are acquired by means of 1" interferential filters with 10 nm bandwidth (Balzers, Germany) at about 10 nm wavelength interval from 400 nm to 700 nm. Each monochromatic image undergoes automatic segmentation (adaptive thresholding and region growing algorithms) (Coltelli and Gualtieri, 1990) to detect the cell region of interest (ROI) on which the integrated absorbance is calculated.

The high quality inspection probe is made by 19 light-guides that form a bundle at the level of the entrance pupil (Figure 1g) and become vertically aligned at the level of the exit pupil (Figure 1h). Each light-guide acquires the light transmitted by the ROI, and images it onto a diffraction grating (model 52300070, Jobin Yvon, Longjumenau, France) (Figure 1i), which disperses the impinging light into separate wavelengths. The dispersed image of the probe is in turn focused onto a digital slow scan cooled CCD camera (DTA Discovery DS260E, Pisa, Italy, IEEE 1394 interface) (Figure 1j). To perform the microspectrophotometric measurements, the inspection probe is centered on the ROI in such a way that at least 1 or 2 light-guides are positioned on an empty field. The light-guides positioned on the ROI measure the transmitted light intensity (I_t), while those positioned on the empty field measure the incident light intensity (I_i). All the absorption spectra are recorded from 400 nm to 700 nm (step size = 0.5 nm) by measuring the absorbance A (log (Ii/It)) at each wavelength (Evangelista, et al., 2007).

MATLAB R2009b software (MathWorks, NaticK USA) and home-made routines were used for data analysis, image processing and pattern recognition (Gonzalez, et al., 2004).

3. Results and Discussion

In this section we will describe and discuss four experimental cases on which our system has been tested.

3.1. Experimental Case 1: monitoring of Cr^{6+} effect on the photosynthetic apparatus of microalgae

Chromium (Cr) mostly occurs as trivalent ion (Cr^{3+}) with low solubility and reactivity, which confer it low toxicity for living organisms (Katz and Salem, 1994). In oxygen-saturated environment Cr^{3+} oxidizes to Cr^{6+}, which can easily cross cell membranes with highly toxic effects due to the increase of reactive oxygen species (ROS) and reduction of cell antioxidant capacity (Cervantes, et al., 2001; Pinto, et al., 2003; Reed, et al., 1990). In algae and plants Cr^{6+} affects mainly the photosynthetic machinery extremely sensitive to peroxidation (Ali, et al., 2006).

We have analyzed the effects of Cr^{6+} on three fresh water microalgae, *Chlamydomonas reinhardtii*, *Eudorina unicocca* and *Chlorella kessleri* (Figure 2). *Chlamydomonas* is a naked cell; *Eudorina* possesses a mucilage cover, whereas *Chlorella* is surrounded by a cell wall. In order to understand whether these differences correspond to different exclusion mechanisms for heavy metals (chromium in our case), and if these algae can be use as probes or bioremediators (Juarez, et al., 2008; Rodriguez, et al., 2007), we have used *in vivo* microspectroscopy to monitor the degradation of the chlorophylls with the consequent formation of phaeophytins, the magnesium-free derivative of chlorophylls, inside single cells. The spectroscopic contribution of each pigment to the absorption spectrum envelop was calculated by an unsupervised statistical estimation in a fully Bayesian setting, i.e. each component pigment is isolated from a set of known mixtures of the pigments (Bell and Sejnowski, 1995; Cichocki and Amari, 2002; Coltelli, et al., 2016).

In *Chlamydomonas,* the toxic effect is dramatically rapid and the complete pheophinitization of both chlorophyll *a* and *b*, is obtained at Cr^{6+} concentration ≥ 10 μmM. Because *Chlamydomonas* cells lack a protective wall, they cannot cope with the Cr^{6+} damage of their photosynthetic machinery; hence they can be considered an effective bioindicator (Figure 2a).

In *Eudorina*, the toxic effect is gradual and the complete pheophinitization of both chlorophyll *a* and *b* is reached at concentration ≥ 40 μmM. Because *Eudorina* cells are embedded in a mucilage covering, the Cr^{6+} effect is attenuated due to the difficulty of the ions to cross the mucilage barrier (Figure 2b).

In *Chlorella*, chromium up to 40 mM (about one hundred times the limit for total Cr discharge established by US EPA regulations) has almost no effect on the chloroplasts and no pheophinitization is observed. Because *Chlorella* is protected by a robust cell wall, Cr^{6+} entrance in the cell is completely hindered. This wall gives *Chlorella* a high removal capacity of toxic ions, and allows it to survive in highly contaminated environment; hence, *Chlorella* can be considered a useful sorption tool to detoxify contaminated waste water (Figure 2c).

3.2. Experimental Case 2: analysis of the movement parameters of swimming algae

The exact determination of the movement parameters of swimming algae can be a very useful tool to investigate behavioral and physiological aspects of the motility of these cells. A wide variety of natural

processes has been usually investigated by analyzing videotape recordings of microorganisms moving onto a microscope slide (Gualtieri, et al., 1985; Gualtieri, et al., 1988). This digital tracking microscope determines the movement parameters by reconstructing the entire trajectories of swimming microorganisms. This system detects the cells in the frames by means of a labelization procedure, and for each detected cell the trajectories are reconstructed by joining the baricenters in successive frames. However, though this image analysis gives satisfactory results, systems based on video recordings are time consuming; as the number of reconstructed tracks must be high (several thousands) to achieve accurate statistical results, the time necessary for the analysis is a fundamental constraint. Attempts to shorten the time of analysis are offered by systems that simply extract and follow one microorganism at a time in the microscope field, without using videotape recordings (Hader and Lebert, 1985); or by systems that sum successive video frames in a floppy disk and thins the recorded tracks; the process is completed by a tracing procedure that searches for suitable tracks (Kondo, et al., 1988). In a previous version, our system acquired images and stored them in a RAM board at an acquisition rate of 25 frames/s, sufficient for track reconstruction (Gualtieri and Coltelli, 1989b; Gualtieri and Coltelli, 1991); in the present version the acquisition rate increases up to 500 frames/s allowing also the analysis of flagellar movements (Barsanti, et al., 2016).

In order to detect moving algal cells and get rid of other objects, such as debris and dead cells, our system performs a temporal difference between successive frames. To avoid the overlapping of the images of the same alga in successive frames, the delay between two frames can be properly chosen according to the axial speed of the cell (Coltelli, et al., 2008). The segmentation and labelization algorithm applied on the difference image produces a complete description of the algae present in each image of the sequence. Each image is partitioned into a set of regions, i.e. background, cells and debris (segmentation) and all these regions are then identified as single entities (labelization). The complete labelization of an image is a typical recursive procedure and it normally requires backtracks at each point when regions are found to recombine. The algorithm we implemented works in a single pass labelling regions while generating a data structure organized in lists containing the cell features. The algorithm is very fast since it relies on handling the computer memory as if it were an associative memory, thus allowing parallel computation (Coltelli and Gualtieri, 1990). The number of cells present in each difference image sets the length of the list of features generated by the labelization algorithm. Each list contains a pointer that points to a list of features, and the list of features. The features can be chosen according to the problem to be solved; in our case, cell baricenter, cell area, Feret diameter and characteristic color are the most important features for algae identification.

Track reconstruction algorithm generates the tracks of the all the algal cell present in the sample by following each cell in the sequence of images. The tracks are reconstructed joining the cells whose baricenters lay within a prefixed distance range, and whose calculated motion vector form an angle with the forecast motion vector within a prefixed angle value. The track ends when no more barycenter satisfies these conditions. The distance range and the angle value are set on the basis of the swimming parameters on

the algae. When the reconstruction procedure encounters more than one cell that satisfies the selection criteria, the algorithm chooses the cell which allows the construction of the motion vector with the smallest deviation angle from the forecast motion vector. To minimize the problem of intersecting tracks of cells swimming freely under the microscope, we use a low depth of focus, so that the cells swimming in the in-focus layer are not hidden by the cells swimming in the out-of-focus layers. When two or more cells hide each other in the in-focus layer, the algorithm recognizes a cell with an area greater than the average and a single barycenter. This barycenter is used to calculate cell motion vectors and it will be assigned to the cell trajectories whose last motion vectors differs from the forecast vector of a prefixed value. The result of the reconstruction procedure is a list containing the movement parameters of all the swimming algae, required to investigate algae behavior.

The track reconstruction algorithm has been already tested on *Euglena gracilis* to investigate the different behavior of the cells with and without unilateral light stimuli (Gualtieri, et al., 1985; Gualtieri, et al., 1988), and on *Dunaliella salina* stumpy mutant to study the peculiar movement of cells with short flagella (Vismara, et al., 2004). A further demonstration of the potentiality of our system is shown in Figure 3: the movement parameters of the dinoflagellate *Gymnodinium acidotum*, present in an environmental sample and swimming fast and freely onto the slide have been exactly determined and the cell track fully reconstructed. The variation of Feret diameters and gray level intensities of the cell has been used to calculate rotational velocities, whereas the barycenter variations have been used to calculate longitudinal velocity. In this example, the image difference procedure has been disabled.

3.3. Experimental Case 3: spectroscopic dynamics of Euglena gracilis photoreceptor functioning

Euglena gracilis possesses a photoreceptive apparatus consisting of a crystalline photoreceptor and a shading eyespot formed by carotenoids globules (Barsanti et al. 2008). To understand how this photoreceptive system works, the spectroscopic features of *Euglena* photoreceptor has been investigated by fluorescence microscopy. The fluorescence images were acquired at two different excitation wavelengths and at the fastest time resolution. These images were stored in the frame memory using panning, scrolling and storing operations performed during the frame acquisition (Gualtieri and Coltelli, 1989; Gualtieri and Coltelli, 1991). Segmentation and labelization procedures were applied to each fluorescence image to automatically select and measure the integrated emission of the photoreceptor. The values of integrated fluorescence intensities versus time demonstrated that the photoreceptor undergoes a photocycle between two thermic stable states A and B, i.e. it possesses optical bistability (Barsanti, et al., 1997). The series of structural changes that *Euglena* photoreceptive protein(s) undergo in response to light during the photocycle were investigated by means of *in vivo* microspectrophotometry, which performs the continuous absorption spectra measurements of the two stable states, and *in vivo* digital microscopy, which calculates the integrated optical density of images of the photoreceptor acquired at selected wavelengths during the photocycle.

The spectra of the states A and B, measured by microspectrophotometry and digital microscopy, were superimposable. The state A shows a band centered at 498 nm, the state B shows a band centered at 462 nm with a blue shift of 36 nm (Barsanti, et al., 2009). Figure 4a shows the image of the photoreceptor of *Euglena* (framed region) recognized as an almond-shaped dark-gray organelle inside the apical part of the cell. The upper part of Figure 4b shows the absorption spectra of state A (black line) and state B (gray line) measured by microspectrophotometry, and the discrete spectrum measured by digital microscopy (empty circles). The lower part of Figure 4b shows the optical density images of the photoreceptor: the direct visualization of the different absorbance level of the organelle (the darker the tone the higher the absorbance) and the shift between the spectra of the states A and B are clearly visible.

The results of these measurements highlight the photochromic behavior of the photoreceptor of *Euglena*, and state that its photoreceptive proteins possess strong spectroscopic similarities with rhodopsin-like proteins (Barsanti, et al., 2000; Barsanti, et al., 2012; Mercatelli, et al., 2009).

3.4. Experimental Case 4: a water monitoring station for algal identification

Algae are valuable indicators of environmental water quality because they react early, strongly and predictably both in species composition and densities to changing water conditions (nutrient enrichment, organic and inorganic contamination, increases in suspended sediments, and changes in pH or conductivity) (Artiola, et al., 2004; Rai, et al., 2008; Singh, et al., 2013; Wiersma, 2004). Hence, automatic identification and enumeration of microalgae by means of image analysis are powerful tools for monitoring water body conditions and provide early warning signs. Many systems have been developed for these purposes (Blackburn, et al., 1998; Culverhouse, et al., 2006; Embleton, et al., 2003; Gorsky, et al., 1989; Kamath, et al., 2005; Mosleh, et al., 2012; Rodenacker, et al., 2006; Santhi, et al., 2013; Verikas, et al., 2012; Yao, et al., 2007), and in the following we will shortly describe the system built by our group (Coltelli, et al., 2013; Coltelli et al., 2014). Our system combines automatic image segmentation, in-focus algae detection, recognition and feature determination, performs algae classification and measures cell concentration in multi-algal samples, according to the following flow of operations:

1. Acquisition of microscope fields
2. Detection and recognition of algae and objects other than algae
3. Determination of algae characteristic color and removal of overlapping and out-of-focus cells
4. Grouping and identification of algae

1. *Acquisition of microscope fields*. Different microscope fields of slides containing multi-algal samples are acquired with adjusted white balance following a boustrophedonic path (Coltelli et al., 2014)). The purpose of this step is to obtain well-focused images with the highest information content.

2. *Detection and recognition of algae and objects other than algae*. For an accurate detection, identification, classification and enumeration of algae, all the objects other than algal cells must be detected and discarded in the successive operations. Therefore, acquired images undergo objects segmentation, cell recognition and

invariance transformation for translation, rotation and scaling. The algorithm calculates the points of the cell contours, the centroid distance spectrum, the dissimilarity measurement, and other features such as center of gravity coordinates, area, Feret diameters, extinction, etc. for a total of 94 morphological and densitometric features (Coltelli et al., 2013; Coltelli et al., 20134).

3. *Determination of algae characteristic color and removal of overlapping and out-of-focus cells*

All the objects detected and recognized as algae undergo characteristic color determination (i.e. the color that represents the pigment signature of the taxonomic group each alga belongs to). For this purpose, image colors are converted from the RGB color space into the L*c*h* color space (Lightness, chroma, and hue), and the color histogram calculated. Using a maximum likelihood estimate this histogram is fitted in a mixture of multivariate Gaussian distribution. In the case of in-focus cells, the fitted color histogram shows two bands, one corresponding to the color of the chloroplast and the other corresponding to the color of the background. In case of out-of-focus cells, the fitted color histogram shows more than two bands, two or more corresponding to the colors of the chloroplast compartment and one corresponding to the color of the background (Coltelli et al., 2014).

4. *Grouping and identification of algae*. The features of objects recognized as algae are organized in vectors, which are grouped in classes by means of an Unsupervised Self-Organizing Map (SOM) consisting of a bi-dimensional structure of regularly spaced connected elements called neurons (Sap and Mohebi, 2008). The SOM algorithm organizes the feature vectors into homogeneous groups. To define the true boundaries of each group, segmentation procedure is applied, which produces a partitioned map with as many regions as the real taxonomic groups of algae. Knowing the number of cells belonging to each group is, it is possible to calculate the concentration of the different algae in the samples.

Figure 5 shows the output of the four operations. Frame 5a shows a typical environmental sample containing in-focus algae, out-of-focus algae, cells partly overlapping the slide border, empty dead cells, detritus, bacteria and debris. All the objects present in the image have been recognized and framed with different colors. The green framed object is the only one recognized as "alga"; this cell is shown magnified in frame 5b. Frames 5c-5f show the extracted features of the cell, i.e. contour and Feret diameter (5c); normalized and invariant contour (5d); centroid distance spectrum with the dissimilarity measure (5e); three-dimensional color histogram showing only the chloroplast color component (5f); SOM group (32) and taxonomic assignment of the alga (*Symbiodinium*-like) represented only by its characteristic color (5g). The assignment has been validated by an expert phycologist. It is worthwhile to emphasize that this image (5g) is barely distinguishable from the original image shown in Figure 5b.

Our system achieves accuracy values higher than those obtained by other identification and classification methods, and with taxonomic accuracy up to 99%, comparable to that obtained by phycology expertise (Coltelli et al., 2014).

References

Ali NA, Dewez D, Didur O, Popovic R. (2006). Inhibition of photosystem II photochemistry by Cr is caused by the alteration of both D1 protein and oxygen evolving complex. Photosynthesis Research 89(2): 81-87.

Artiola J, Pepper IL, Brusseau ML, editors. (2004). Environmental Monitoring and Characterization Elsevier Science & Technology Books.

Barsanti L, Passarelli V, Walne PL, Gualtieri P. (1997). In Vivo Photocycle of the *Euglena gracilis* Photoreceptor. Biophysical Journal 72 (2): 545-553.

Barsanti L, Passarelli V, Walne PL, Gualtieri P. (2000). The photoreceptor protein of *Euglena gracilis*. Febs Letter 482 (3): 247 - 251

Barsanti L, Evangelista V, Frassanito AM, Vesentini N, Passarelli V, Gualtieri P. (2007). Absorption microspectroscopy, theory and applications in the case of the photosynthetic compartment. Micron 38(3): 197-213.

Barsanti L, Coltelli P, Evangelista V, Passarelli V, Frassanito AM, Vesentini N, Gualtieri P. (2008). Low-resolution characterization of the 3D structure of the *Euglena gracilis* photoreceptor. Biochemical and Biophysical Research Communications 375: 471–476.

Barsanti L, Coltelli P, Evangelista V, Passarelli V, Frassanito AM, Vesentini N, Santoro F, Gualtieri P. (2009). In Vivo Absorption Spectra of the Two Stable States of the *Euglena* Photoreceptor Photocycle. Photochemistry and Photobiology 85(1): 304-312.

Barsanti L, Evangelista V, Passarelli V, Frassanito AM, Gualtieri P. (2012). Fundamental questions and concepts about photoreception and the case of *Euglena gracilis*. Integrative Biology 4(1): 22-36.

Barsanti L, Gualtieri P. (2014). Algae: Anatomy, Biochemistry and Biothecnology. Boca Raton, FL (USA): CRC Press.

Barsanti L, Coltelli P, Evangelista V, Frassanito AM, Gualtieri P. (2016). Swimming patterns of the quadriflagellate *Tetraflagellochloris mauritanica* (Chlamydomonadales, Chlorophyceae). Journal of Phycology 52(2): 209-218.

Bell AJ, Sejnowski TJ. (1995). An Information-Maximization Approach to Blind Separation and Blind Deconvolution. Neural Computation 7(6): 1129-1159.

Blackburn N, Hagström A, Wikner J, Cuadros-Hansson R, Bjørnsen PK. (1998). Rapid Determination of Bacterial Abundance, Biovolume, Morphology, and Growth by Neural Network-Based Image Analysis. Applied and Environmental Microbiology 64(9): 3246-3255.

Carvalho L, McDonald C, de Hoyos C, Mischke U, Phillips G, Borics G, Poikane S, Skjelbred B, Solheim AL, Van Wichelen J, Cardoso AC. (2013). Sustaining recreational quality of European lakes: minimizing the health risks from algal blooms through phosphorus control. Journal of Applied Ecology 50(2): 315-323.

Cervantes C, Campos-García J, Devars S, Gutiérrez-Corona F, Loza-Tavera H, Torres-Guzmán JC, Moreno-Sánchez R. (2001). Interactions of chromium with microorganisms and plants. FEMS Microbiology Reviews 25(3): 335-347.

Cichocki A, Amari S-i. (2002). In: Adaptive Blind Signal and Image Processing. New York: John Wiley & Sons, Ltd.

Coltelli P, Gualtieri P. (1990). A procedure for the extraction of object features in microscope images. International Journal of Bio-Medical Computing 25(2-3): 169-176.

Coltelli P, Evangelisti M, Evangelista V, Gualtieri P. (2008). An automatic real-time system for the determination of translational and rotational speeds of swimming micro-organisms. Int. J. of Signal and Imaging Systems Engineering 1: 25-29.

Coltelli P, Barsanti L, Evangelista V, Frassanito AM, Passarelli V, Gualtieri P. (2013). Automatic and real time recognition of microalgae by means of pigment signature and shape. Environmental Science: Processes & Impacts 15(7): 1397-1410.

Coltelli P, Barsanti L, Evangelista V, Frassanito AM, Gualtieri P. (2014). Water monitoring: automated and real time identification and classification of algae using digital microscopy. Environmental Science, Processes & Impacts 16(11): 2656-2665.

Coltelli P, Barsanti L, Evangelista V, Frassanito AM, Gualtieri P. (2016). Reconstruction of the absorption spectrum of an object spot from the color values of the corresponding pixel(s) in its digital image: the challenge of algal colors. Journal of Microscopy doi: 10.1111/jmi.12445

Culverhouse PF, Williams R, Benfield M, Flood PR, Sell AF, Mazzocchi MG, Buttino I, Sieracki M. (2006). Automatic image analysis of plankton: future perspectives. Marine Ecology Progress Series 312: 297-309.

Embleton KV, Gibson CE, Heaney SI. (2003). Automated counting of phytoplankton by pattern recognition: a comparison with a manual counting method. Journal of Plankton Research 25(6): 669-681.

Evangelista V, Passarelli V, Barsanti L, Gualtieri P. (2003). Fluorescence Behavior of *Euglena* Photoreceptor. Photochemistry and Photobiology 78(1): 93-97.

Evangelista V, Frassanito AM, Passarelli V, Barsanti L, Gualtieri P. (2006). Microspectroscopy of the Photosynthetic Compartment of Algae. Photochemistry and Photobiology 82(4): 1039-1046.

Evangelista V, Evangelisti M, Barsanti L, Frassanito AM, Passarelli V, Gualtieri P. (2007). A polychromator-based microspectrophotometer. International Journal of Biological Sciences 3(4): 251 - 256.

Evangelista V, Barsanti L, Frassanito AM, Passarelli V, Gualtieri P. (2008). Algal toxins : nature, occurrence, effect and detection. Dordrecht: Springer.

Gonzalez RC, Woods RE, Eddins SL. (2004). Digital Image Processing using MATLAB. London: Pearson/Prentice Hall.

Gorsky G, Guilbert P, Valenta E. (1989). The Autonomous Image Analyzer - enumeration, measurement and identification of marine phytoplankton Marine Ecology Progress Series 58: 133-142.

Gualtieri P, Colombetti G, Lenci F. (1985). Automatic analysis of the motion of microorganisms. Journal of Microscopy 139(1): 57-62.Gualtieri P. (1991). Microspectroscopy of photoreceptor pigments in flagellated algae. Critical Reviews in Plant Sciences 9(6): 475-495.

Gualtieri P, Ghetti F, Passarelli V, Barsanti L. (1988). Microorganism track reconstruction: An image processing approach. Computers in Biology and Medicine 18(2): 57-63.

Gualtieri P, Passarelli V, Barsanti L. (1989a). A simple instrument to perform 'in vivo' absorption spectra of pigmented cellular organelles. Micron and Microscopica Acta 20(2): 107-110.

Gualtieri P, Coltelli P. (1989a). A digital microscope for real time detection of moving microorganisms. Micron and Microscopica Acta 20(2): 99-105.

Gualtieri P, Coltelli P. (1991). An image-processing system, motion analysis oriented (IPS-100), applied to microscopy. Comput Methods Programs Biomed 36(1): 15-25.

Gualtieri P. (1992). Molecular biology in living cells by means of digital optical microscopy. Micron and Microscopica Acta 23(3): 239-257.

Häder D-P, Lebert M. (1985). Real time computer-controlled tracking of motile microorganisms. Photochemistry and Photobiology 42(5): 509-514.

Juarez AB, Barsanti L, Passarelli V, Evangelista V, Vesentini N, Conforti V, Gualtieri P. (2008). In vivo microspectroscopy monitoring of chromium effects on the photosynthetic and photoreceptive apparatus of *Eudorina unicocca* and *Chlorella kessleri*. J Environ Monit 10(11): 1313-8.

Kamath SB, Chidambar S, Brinda BR, Kumar MA, Sarada R, Ravishankar GA. (2005). Digital image processing—an alternate tool for monitoring of pigment levels in cultured cells with special reference to green alga *Haematococcus pluvialis*. Biosensors and Bioelectronics 21(5): 768-773.

Katz SA, Salem H. (1994). The Biological and Environmental Chemistry of Chromium. New York: VCH Publishers.

Kondo T, Kubota M, Aono Y, Watanabe M. (1989). A Computerized Video System to Automatically Analyze Movements of Individual Cells and Its Application to the Study of Circadian Rhythms in Phototaxis and Motility in *Chlamydomonas* reinhardtii. In: Cell Dynamics: Cytoplasmic Streaming Cell Movement—Contraction and Migration Cell and Organelle Division Phototaxis of Cell and Cell Organelle. Tazawa M, editor. Vienna: Springer Vienna. pp 185-191.

Mercatelli R, Quercioli F, Barsanti L, Evangelista V, Coltelli P, Passarelli V, Frassanito AM, Gualtieri P. (2009). Intramolecular photo-switching and intermolecular energy transfer as primary photoevents in photoreceptive processes: the case of *Euglena gracilis*. Biochemical and Biophysical Research Communications 385: 176–180.

Mosleh M, Manssor H, Malek S, Milow P, Salleh A. (2012). A preliminary study on automated freshwater algae recognition and classification system. BMC Bioinformatics 13(Suppl 17): S25.

Pinto E, Sigaud-kutner TCS, Leitão MAS, Okamoto OK, Morse D, Colepicolo P. (2003). Heavy metal–induce oxidative stress in algae. Journal of Phycology 39(6): 1008-1018.

Rai UN, Dubey S, Shukla OP, Dwivedi S, Tripathi RD. (2008). Screening and identification of early warning algal species for metal contamination in fresh water bodies polluted from point and non-point sources. Environmental Monitoring and Assessment 144(1-3): 469-481.

Reed RH, Gaad GM. (1990). Metal tolerance in eukaryotic and prokaryotic algae. In: Heavy metal tolerance in plants: evolutionary aspects. Shaw AJ, editor. Boca Raton: CRC Press. pp 105-108.

Rodenacker K, Hense B, Jütting U, Gais P. (2006). Automatic analysis of aqueous specimens for phytoplankton structure recognition and population estimation. Microscopy Research and Technique 69(9): 708-720.

Rodriguez MC, Barsanti L, Passarelli V, Evangelista V, Conforti V, Gualtieri P. (2007). Effects of chromium on photosynthetic and photoreceptive apparatus of the alga *Chlamydomonas reinhardtii*. Environmental Research 105(2): 234 - 239.

Santhi N, Pradeepa C, Subashini P, Kalaiselvi S. (2013). Automatic Identification of Algal Community from Microscopic Images. Bioinformatics and Biology Insights 7(3911-BBI-Automatic-Identification-of-Algal-Community-from-Microscopic-Images.pdf): 327-334.

Sap MNM, Mohebi E. (2008). Hybrid Self Organizing Map for Overlapping Clusters. International Journal of Signal Processing, Image Processing and Pattern Recognition 1: 11-20.

Singh UB, Ahluwalia AS, Sharma C, Jindal R, Thakur RK. (2013). Planktonic indicators: a promising tool for monitoring water quality (early-warning signals). Eco. Env. & Cons. 19(3): 793-800.

Verikas A, Gelzinis A, Bacauskiene M, Olenina I, Olenin S, Vaiciukynas E. (2012). Automated image analysis- and soft computing-based detection of the invasive dinoflagellate Prorocentrum minimum (Pavillard) Schiller. Expert Systems with Applications 39(5): 6069-6077.

Vismara R, Verni F, Barsanti L, Evangelista V, Gualtieri P. (2004). A short flagella mutant of *Dunaliella salina* (Chlorophyta, Chlorophyceae). Micron 35(5): 337-344.

Walker RF, Ishikawa K, Kumagai M. (2002). Fluorescence-assisted image analysis of freshwater microalgae. Journal of Microbiological Methods 51(2): 149-162.

Wiersma GB, editor. (2004). Environmental Monitoring. Boca Raton: CRC Press.

Yao Z, Fei M, Li K, Kong H, Zhao B. (2007). Recognition of blue-green algae in lakes using distributive

genetic algorithm-based neural networks. Neurocomputing 70(4–6): 641-647.

Zieler HW. (1972). The optical performance of the light microscope Part.1. London: Microsope Publications Ltd. 102 p.

Figure legends

Figure 1. The home-made microscopy set-up. a) 100W tungsten lamp; b) condenser; c) microscope stage; d) objective; e) two-ports binocular tube; f) CCD or CMOS camera; g) entrance pupil of the optical fiber showing the light-guides bundle; h) exit pupil of the optical fiber showing the aligned light-guides; i) diffraction grating; j) slow scan cooled CCD camera.

Figure 2. a) Left panel: *Chlamydomonas* untreated cell; absorption spectrum of the chloroplast of an untreated cell (black line) and absorption spectrum of each isolated pigment (color lines) are shown together with their maxima. Right panel: 10 μM Cr treated cell; absorption spectrum of the chloroplast of a 10 μM Cr treated cell (black line), and absorption spectrum of each isolated pigment (color lines) are shown together with their maxima.
b) Left panel: *Eudorina* untreated cell; absorption spectrum of the chloroplast of an untreated cell (black line), and absorption spectrum of each isolated pigment (color lines) are shown together with their maxima.
Right panel: 40 μM Cr treated cell, absorption spectrum of the chloroplast of a 40 μM Cr treated cell (black line), and absorption spectrum of each isolated pigment (color lines) are shown together with their maxima.
c) Left panel: *Chlorella* untreated cell; Absorption spectrum of the chloroplast of an untreated cell (black tick line), and absorption spectrum of each isolated pigment (color lines) are shown together with their maxima.
Right panel: 40 mM Cr treated cell, absorption spectrum of the chloroplast of a 40 mM Cr treated cell (black tick line), and absorption spectrum of each isolated pigment (color lines) are shown together with their maxima.

Figure 3. Overlaid images of a *Gymnodinium acidotum* cell during motion. Contours and barycenters are marked on each image. The plots of the reconstructed cell path, the variation of minimum Feret diameters and the variation of gray level intensity are shown below.

Figure 4. a) Digital image of the apical portion of an *Euglena* cell; the photoreceptor is clearly visible inside the framed region as an almond-shaped dark-gray organelle. b) Absorption spectra of state A (black line) and state B (gray line) of the photoreceptor measured by microspectrophotometry; the superimposed dots correspond to the measurement performed by digital microscopy at 12 selected wavelengths. The corresponding optical density images are shown in the rows below.

Figure 5. Result of algal identification procedure. a) Acquired image of an environmental sample: objects identified as bacteria, detritus, and debris are magenta-framed; objects identified as algal cells partly overlapping the slide border are blue-framed; objects identified as empty dead algae, overlapping cells, and out-of-focus cells are yellow-framed; objects identified as in-focus algae are green-framed; b) magnified image of the in-focus alga of frame 5a; c) yellow contour and maximum Feret diameter of the alga; d) normalized and invariant contour; e) centroid distance spectrum, with the dissimilarity measure; f) three-dimensional color histogram showing only the chloroplast color component; g) SOM group and taxonomic assignment of the alga represented only by its characteristic color.

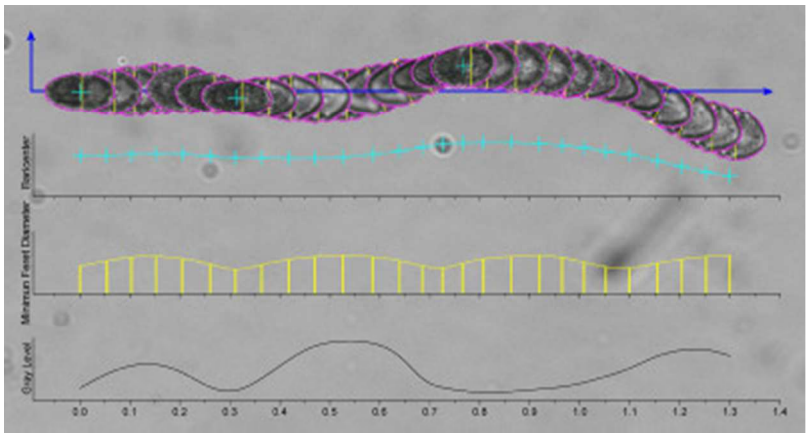

141x75mm (72 x 72 DPI)

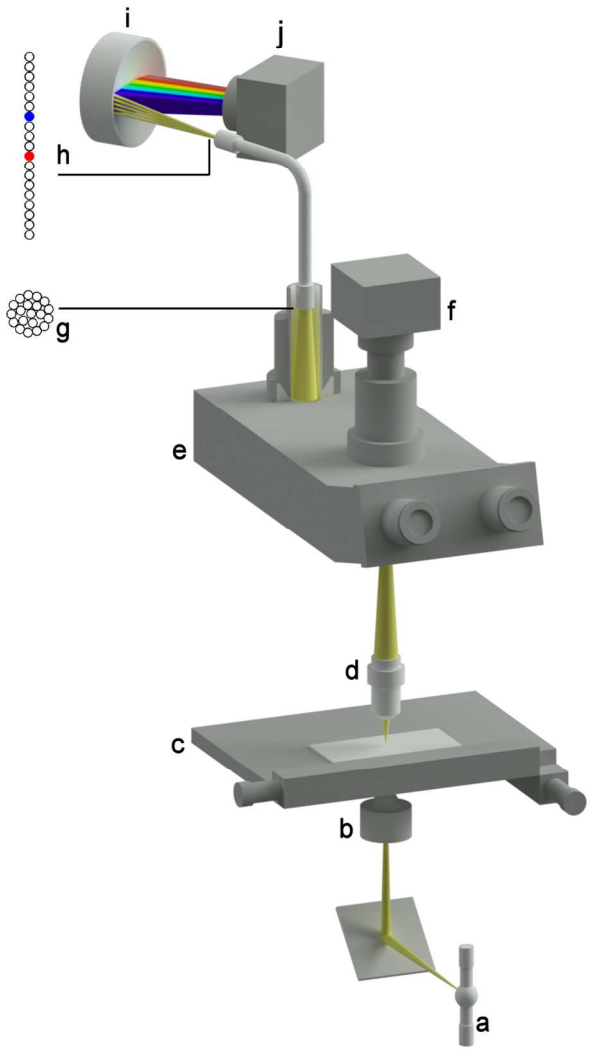

Figure_1

127x181mm (300 x 300 DPI)

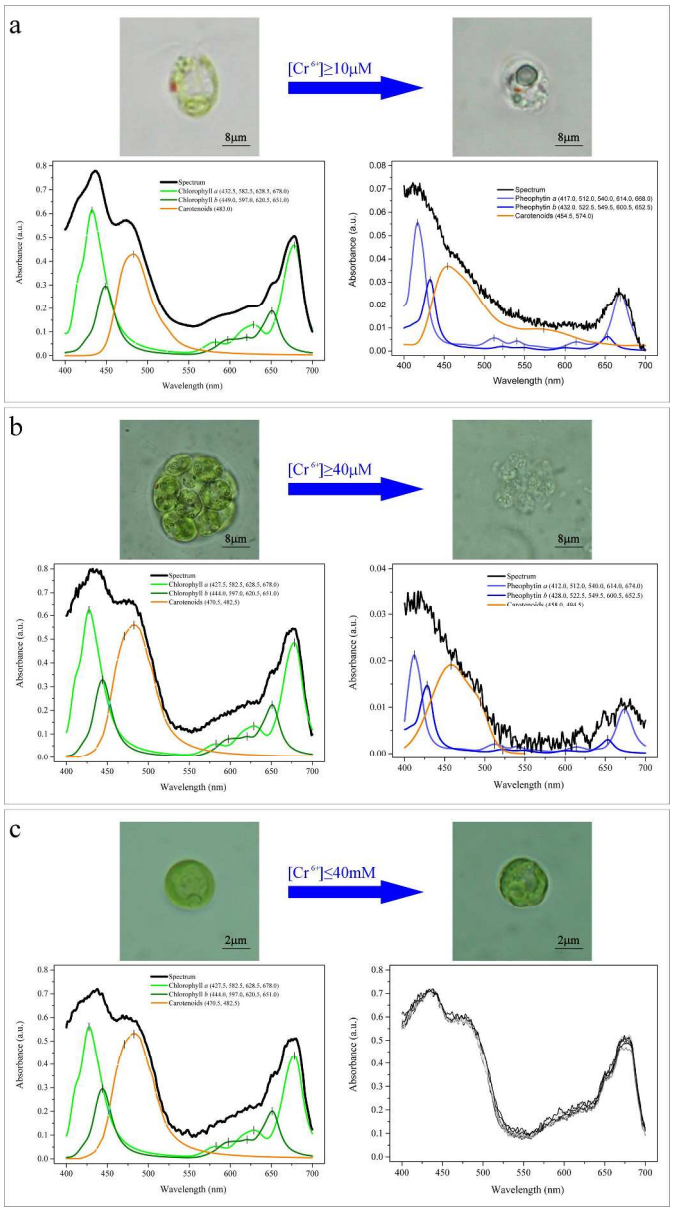

Figure_2

213x385mm (300 x 300 DPI)

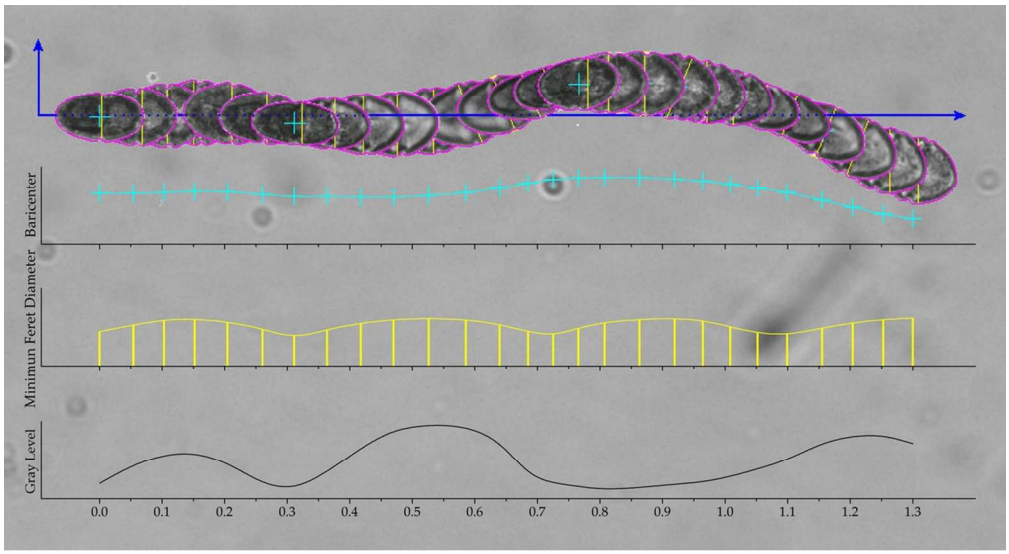

Figure_3

103x56mm (300 x 300 DPI)

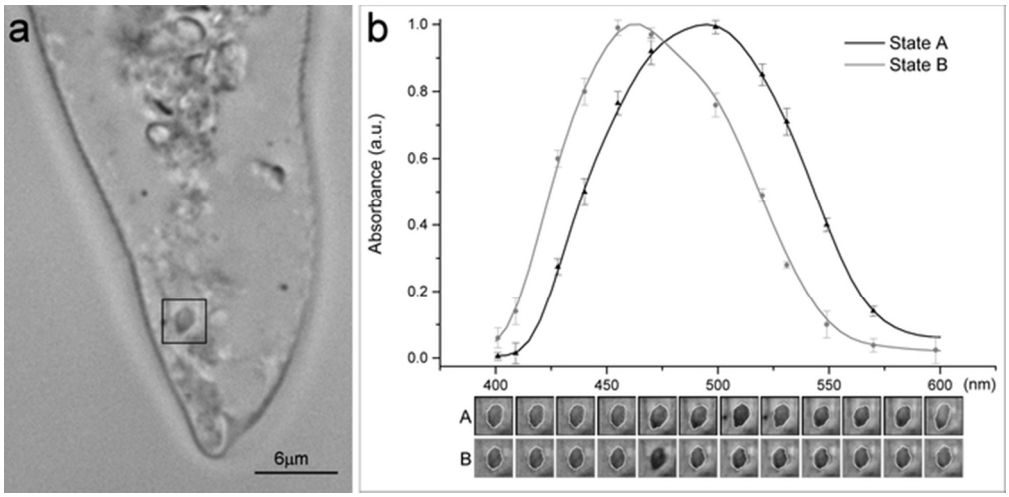

Figure_4

59x28mm (300 x 300 DPI)

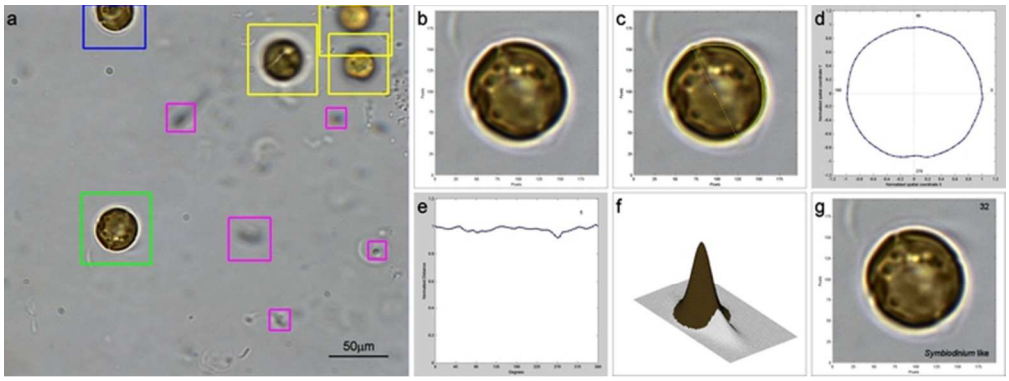

Figure_5

62x23mm (300 x 300 DPI)